3D ANALYSIS OF THE RING CURRENT, FOR THE 20 APRIL 2002 EVENT, USING ENAs IMAGE INVERSIONS (IMAGE/HENA) AND THE CURLOMETER TECHNIQUE (CLUSTER/FGM DATA)

Claire Vallat [(1)], Iannis Dandouras [(2)], Pontus C:Son Brandt [(3)], Ed Roelof [(3)], Don Mitchell [(3)], Malcolm Dunlop [(4)], Elizabeth Lucek [(5)], André Balogh [(5)],Henri Rème [(2)].

(1) ESTEC ESA, Noordwijk, The Netherlands, email:cvallat@rssd.esa.int
(2) Centre d'Etude Spatiale des Rayonnements, Toulouse, France
(3) Applied Physics Laboratory, Johns Hopkins University, Maryland, USA
(4) Rutherford Appleton Laboratory, Didcot, UK
(5) Blackett Laboratory, Imperial College, London, UK

ABSTRACT

The inner magnetosphere's electric currents configuration and mapping is one of the keys for understanding current loop closure inside the whole magnetosphere. Development of the ring current as a function of geomagnetic activity is still one of the most crucial aspects about this region.
A method to estimate the current density vector is the multi-spacecraft curlometer technique, which is based on Maxwell-Ampere's law application. This requires the use of four point magnetic field high-resolution measurements. The FGM experiment on board the four Cluster spacecraft allows for the first time an instantaneous calculation of the magnetic field gradients and thus a measurement of the local current density.
Moreover, inversions of Energetic Neutral Atom (ENA) images obtained by IMAGE/HENA can provide the global ion distribution in the equatorial plane, and thus an estimate of global partial pressures distribution. By using a realistic magnetic field model, a part of the global pressure-driven current system can be computed and used to put the local results of the curlometer technique into context. Using these two complementary methods (curlometer technique using in-situ measurements and neutral atom image inversion using remote sensing data), an instantaneous 3D mapping of the current can be made.
The ring current distribution has been studied for the 20 April 2002 storm event. During the early recovery phase of this storm (Dst~ - 101 nT; Kp=6), Cluster was crossing the perigee at R~ 4 R_E in the evening sector (MLT~21). The Cluster constellation provided a direct measure of the local current density, by applying the curlometer technique. Simultaneously, Cluster was situated inside the HENA/IMAGE field-of view, allowing a validation of the ion fluxes obtained from HENA/IMAGE image inversions. Our analysis reveals the existence of an important local current density (~ 30 nA/m^2), even if the Cluster spacecraft are situated slightly duskward of the ring current bulk, as shown by the HENA image inversion. The curlometer results reveal also the existence of an asymmetry between the two hemispheres, characterized by a southward orientation of the current at the equator.

1. INTRODUCTION

Efforts have been made during the last thirty years to get a global mapping of the ring current, using various methods together with experimental data. In reference [1] in-situ ion measurements from AMPTE Charged Particle Explorer spacecraft were used to calculate the pressure gradient, and then get an estimate of the perpendicular current in the equatorial plane. This allowed to establish a 2D profile of the current in the equatorial plane. However, this method only provides the perpendicular component of current, and requires also an assumption of stationarity between two points of measurements.
Using magnetic field measurements from a single spacecraft, it is also possible to estimate, by using a magnetic field model as reference, the magnetic field perturbation ΔB created by the current. This method was used to provide the first mapping of the ring current morphology and of the different current systems [2]. But using this method requires, together with an assumption of stationarity, the use of magnetic field and current morphology models.
The Cluster mission have allowed, for the first time, to reduce the inaccuracies of the current density estimate by applying the curlometer technique to multi-spacecraft data ([3], [4], [5], [6]) reducing thus the assumption of stationarity. As a consequence, measurements of the current density permitted a mapping of the ring current, in strength and in orientation, along the Cluster orbit [7].
Moreover, a new method of Energetic Neutral Atoms image inversions [8][9] has been validated using in-situ measurements [10]. This method provides a unique

Proceedings Cluster and Double Star Symposium – 5th Anniversary of Cluster in Space, Noordwijk, The Netherlands, 19 - 23 September 2005 (ESA SP-598, January 2006)

opportunity to rebuild the ion distribution in the equatorial plane from the Energetic Neutral Atom distribution. This latter population is issued from charge exchange between the ring current energetic ions and the exospheric neutral atoms.
In this paper, the 20 April 2002 storm time event is studied. For this event, the Cluster inter spacecraft distances allowed an accurate measurement of the current density using the curlometer technique, and the IMAGE spacecraft provided a global view of the Energetic Neutral Atom distribution.
The former method will permit to study the latitudinal evolution of the current (along the Cluster polar orbit) whereas the latter one will provide an equatorial ion distribution mapping. These two complementary sets of measurements will allow an instantaneous global 3D mapping of the ring current in the entire inner magnetosphere.

2. CURLOMETER TECNHIQUE

The curlometer technique provides a unique opportunity to estimate the instantaneous current density using four-point measurements of the magnetic field. The method is based on Maxwell-Ampere's law:

$$\mu_0 \vec{J} = \nabla \times \vec{B} - \varepsilon_0 \mu_0 \frac{\partial \vec{E}}{\partial t} \qquad (1)$$

It assumes stationarity in the region of interest ($\frac{\partial \vec{E}}{\partial t} = 0$, i.e. assuming field does not vary on time scales of the spacecraft motion). To apply this method to experimental data, all measurement points must be situated inside the same current sheet. Moreover, various parameters can affect the current density estimate. For Cluster's passes in the ring current, these parameters have been listed and their influence on the current density estimate has been studied in detail [7]. It was shown that, for inter spacecraft separations up to 250 km at perigee, the inaccuracy on the current density estimate was less than 20%. Moreover, this error was mainly carried by the Jz component, corresponding to the component perpendicular to the ring current near the Equator.
As a consequence, under appropriate conditions, the curlometer technique applied to simultaneous points of measurements of the magnetic field can provide an estimate of the instantaneous current density vector, in strength as well as in orientation.

3. IMAGE INVERSION: CONSTRAINED LINEAR METHOD

Ring current ions often interact with cold exospheric neutrals atoms (~1000K) to create energetic neutral atoms (ENAs). The energy of the incident ions is almost entirely transferred to the charge exchange produced ENAs, which then propagate along nearly rectilinear ballistic trajectories. The straight-line paths of the energetic neutral atoms suggest that they can be used to form an image of the ENA emitting regions, mostly corresponding to the ring current region [11].
ENA images thus contain quantitative information of the magnetosphere-exosphere interaction processes on a global scale. Thus, ENAs can be used like photons in order to form an image of the energetic ion distribution. Based on that, a linear inversion technique has been developed (see [8]).
The count in each pixel of an ENA image, C_i , can be represented by the measurement equation:

$$C_i = \int_0^{\infty} \int_0^{\infty} \int_0^{2\pi} \int_0^{\pi} \sin\varepsilon A_i(\varepsilon, \beta, E, t)\, j_{ena}\, d\varepsilon d\beta dE dt \qquad (2)$$

where A_i is the response of the pixel i to an ENA intensity j_{ena} at time t, energy E and angular position ε and β. The ENA intensity from charge exchange can be written as

$$j_{ena} = \int_0^{Se} n^H(s)\sigma_H^{10}(E)\, j_{ion}(s,E)ds + j^e_{ena}(s_e) \qquad (3)$$

where s is the distance along the line of sight determined by ε and β, n^H is the number density of hydrogen, σ_H^{10} is the charge exchange cross section for protons on hydrogen and j_{ion} is the ion flux. The second term j^e_{ena} is the contribution of ENA flux from the interaction between the ring current and the Oxygen of the upper atmosphere at the exobase. The limit of integration, s_e, is either the point where the line of sight first intersects the exobase, or $+\infty$ for lines of sight with no such intersection.
Using a constrained linear inversion technique [8], and using a magnetic field model [12] and an exospheric model [13], one can estimate J_{ion} as:

$$J_{ion} = (K^T \sigma_C^{-2} K + \gamma H)^{-1} K^T \sigma_C^{-2} C \qquad (4)$$

which, for appropriate values of γ and H, has a unique solution. Solutions of this form have been treated extensively by other authors (see for example [14], [15] and [16]). This method can thus provide a global image of the equatorial ion distribution in the ring current region.

4. MISSION AND INSTRUMENTATION

4.1 In-situ measurements by CLUSTER

The Cluster orbit parameters [17] allow the constellation to cross the ring current region from South to North during every perigee pass, and to obtain its latitudinal profile. Moreover, due to the orbit precession of the spacecraft over the year, all magnetic local times can be studied. As a consequence, a sampling of the ring current region at $r \sim 4\ R_E$ (Cluster perigee distance), over all MLT and latitudinal sectors, is feasible.
Onboard each spacecraft, eleven experiments are allowing measurements of the main plasma parameters, together with the electric and magnetic fields. Among others, two ion spectrometers (HIA and CODIF) as well as a fluxgate magnetometer (FGM) are present.

4.1.1 CIS

The Cluster Ion Spectrometer experiment consists of two complementary ion sensors, the COmposition and DIstribution Function analyzer (CODIF) and the Hot Ion Analyzer (HIA). CODIF, which gives a mass per charge composition with a 22.5° angular resolution, is capable of measuring the full three dimensional ion distribution of the major ion species, from thermal energies (~1 eV) to about 40 keV, with one spacecraft spin (4 seconds) time resolution [18]. HIA does not offer mass resolution but has a better angular resolution (5.6°) that is adequate for ion beam and solar wind measurements.

4.1.2 FGM

The FGM experiment is constituted by two triaxial fluxgate magnetometers and an onboard data-processing unit. High vector sample rates (up to 67 vectors.s^{-1}) at high resolution (up to 8 pT) allow a precise measurement of the ambient magnetic field. The magnetic field component along the spin axis (which is almost perpendicular to the ecliptic) will carry the main part of the error made on the measurement, because offsets in the spin plane measurements are easily removed by noting spin-period oscillations. In addition to the on-ground calibrations made to determine the expected maximal offset on each spacecraft (up to 0.1 nT), in-flight calibrations of the magnetometers are regularly applied in order to maximise the accuracy of the magnetic filed measurements. A detailed description of the instruments and its performances is given by [19].

The use of Cluster data allows for the first time to apply the curlometer technique to simultaneous magnetic field data, reducing considerably the limitations induced by the current density estimate methods used so far.

4.2 Remote sensing measurements by IMAGE

The IMAGE spacecraft was launched in March 2000 into an elliptical polar orbit with an apogee altitude of 7.2 R_E and a perigee altitude of 1000 km [20]. On board IMAGE, the HENA (High Energy Neutral Atoms) imager is used to determine the velocity, arrival direction and mass of ENAs in the 10-500 keV energy range. From these data it generates images of ENA source regions in the inner magnetosphere with a ~6° angular resolution [21]. The inversion method applied to HENA data can provide estimation of the ion flux and of the equatorial ion distribution responsible for the creation of ENAs observed by HENA.

5. 20 APRIL 2002 EVENT

5.1 Context

During the 20 April 2002 Cluster perigee pass, the Dst index for the interval (up to –101 nT at 18:00 UT) reveals an early recovering storm time period, with a succession of storms. The AE index reached values up to 1000 nT for this period. The Kp value of 6 confirms the high level of activity.

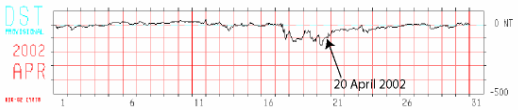

Fig. 1. *Dst index values for April 2002. On the 20 April 2002 storm conditions are observed, while Cluster is passing through perigee. At 18:00 UT, the Dst index was about -101 nT.*

5.2 Observations

5.2.1 In-situ particle measurements: Cluster CIS data

An extended description of the ionic structures observed in the ring current region by the CIS experiment is given in [7]. Here we present a summary of the main features observed.

Cluster spacecraft were crossing perigee in the evening sector (MLT ~ 21 h). Figure 2 presents CODIF and FGM data from SC 4 for the 20 April 2002 event. From top to bottom, it shows, for the proton population,

the energy-time spectrograms (from a few eV to ~ 40 keV) in corrected-for-detection-efficiency count per second, the pitch-angle distribution (for the 27 to 39 keV energy range) in count per sec. from the CIS-CODIF instrument; the magnetic field components, in GSM coordinates (as measured by FGM), the L-shells, invariant latitudes, magnetic latitudes and geocentric distance values. Cluster SC4 entered from the Southern lobe to the plasma sheet boundary layer at 16:30 UT. This transition appears simultaneously with field aligned ions at low energies (not shown) together with very narrow structures observed for energies of 500 eV to a few keV. At lower latitudes (below Ilat = 62°, Southern Hemisphere), this population disappeared, and at about 17:14 UT a high energy population was encountered, showing the entrance into the ring current region. This region is characterized by a change in the pitch angle, from a quite structured (plasma sheet population) to a fully isotropic distribution (freshly injected ring current population).

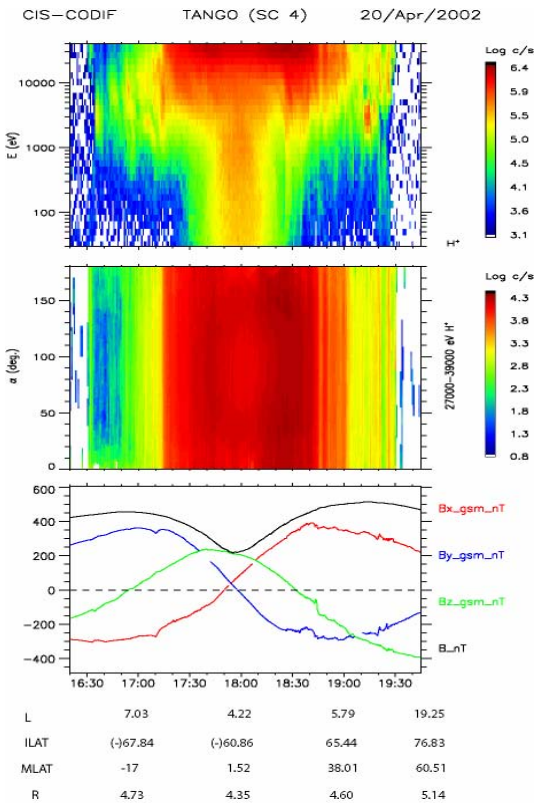

Fig. 2. *Cluster SC4 data for the 20 April 2002 event: H^+ energy-time spectrogram in corrected-for-detection-efficiency count per sec., the pitch-angle distribution (in count per sec.) for the 27 to 39 keV energy range, and the magnetic field components in the GSM coordinate system. L-shell, invariant latitudes, magnetic latitudes and geocentric distances are indicated below. This figure is adapted from [7]*

5.2.2 Magnetic field measurements: curlometer results

The results of the current calculation in the ring current region are presented in figure 3. The three components of the current have been computed in Solar Magnetic coordinates, and then transformed into local cylindrical co-ordinates (upper panel).

While entering in the inner plasma sheet, Cluster/FGM data exhibit a spiky profile for every component of the current density vector, characterizing the presence of non linear gradients inside the tetrahedron formed by the four spacecraft. This is due to the small scale of the current sheets traversed. The transition from the plasma sheet to the ring current is then characterized by a change from a very oscillating current components profile until 17:43 UT (Ilat ~ 61.3°, Southern Hemisphere) to a more regular one. Since the ring current population appears earlier on the particle data (~ 17: 14 UT), we can conclude that between 17: 14 and 17: 43, currents from the Plasma Sheet and the ring current are probably mixed, leading to the presence of 'filamentations' on the current profile. Once the filamentations disappear (after 17: 43 UT), the current profile becomes smoother, even if some small amplitude perturbations due to the high activity level occur, possibly related to multiple particle injections. Filamentations reappear after 18:23 UT. Within these two times (17:43 and 18:23), the dominant current component is, as expected, the J_φ component, with a mean value of J_φ = -24.6 nA.m^{-2} ± 20 %. These data also reveal the large latitudinal extent of the ring current, from Ilat=62.5° (Southern Hemisphere) to Ilat=61.8° (Northern hemisphere), corresponding to about 1.8 R_E in the Z_{gsm} direction.

The $\vec{J}\times\vec{B}$ product (proportional to $(\nabla\vec{P})$), plotted in Figure 3 (middle panel), presents a negative $(\nabla P)_y$ component which indicates that the main part of the current carriers is situated dawnward with respect to the spacecraft. The $(\nabla P)_X$ is oriented earthward, consistent with the observed westward current. Moreover, the inversion of the $(\nabla P)_Z$ component (from positive in the Southern hemisphere to negative ones in the Northern hemisphere) reveals that the ring current bulk is centered on the equatorial plane.

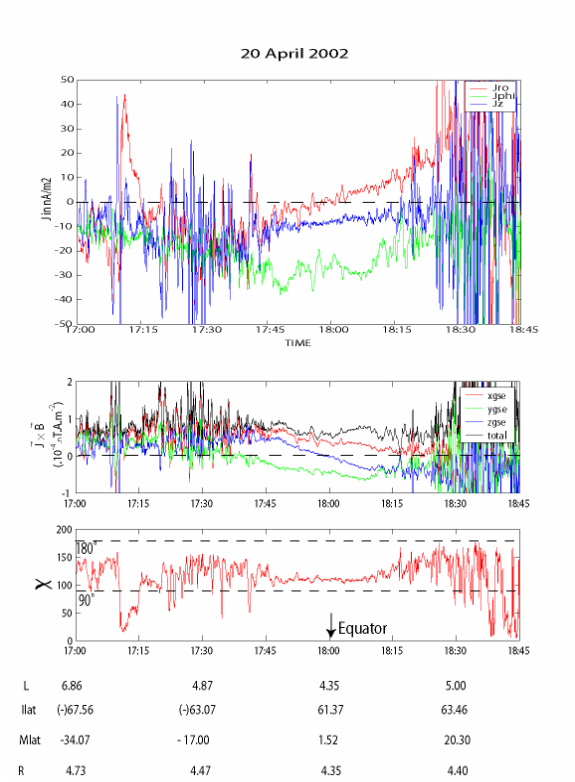

Fig. 3. *Curlometer results for the 20 April 2002 event. From top to bottom: current density in nA.m^{-2} in the local cylindrical coordinate system, pressure gradient (computed from $\vec{J} \times \vec{B}$), and χ angle between local current flow and magnetic field. L-shell, invariant latitudes, magnetic latitudes and geocentric distances are indicated at the bottom of the plot.*

The current orientation (with respect to the magnetic field lines), given by the χ angle ($\chi = \cos^{-1}(\vec{J} \bullet \vec{B} / \|\vec{J}\| \|\vec{B}\|)$), is very stable all over the entire latitudinal extent of the ring current (fig 3, lower panel). Nevertheless the current flow is not centered on 90° as expected (i.e. purely azimuthally flowing current) but rather around 108° all along the traversal (~ 10 nA.m^{-2}). Considering that the inaccuracy on the current density estimate is too small to explain this 18° orientation apart from the expected 90°, this stable negative value can be explained only by the presence, near the equator, of a parallel component of the current density. One assumption is that the component could be the signature of an asymmetry between the ionospheric conductivities of the two hemispheres, which depend on the exposure to the sunlight. Since the exposure is different from one hemisphere to the other, and the closure of the ring current through the two hemispheres is a parallel circuit, this can drive field aligned currents preferentially directed to one of the hemispheres [22],[23].

5.2.3 Remote sensing images: IMAGE/HENA inversions

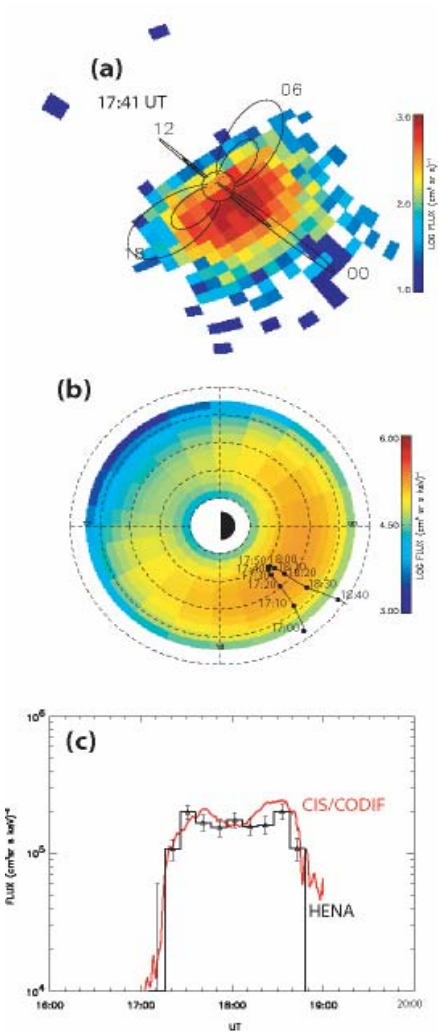

Fig. 4. *IMAGE/ HENA data for April 20, 2002 at 17:41. (a) HENA image of ENAs flux in flux unit (27-39 keV) (b) Equatorial ion distribution (L-MLT system) as deduced from the HENA image using the inversion method, in flux unit. Black dots represent the Cluster position, as projected on the equatorial plane at different times. The Cluster orbit, projected on this plane, is also shown (see text for details). (c) Comparison of the proton fluxes (27-39 keV) as obtained by HENA image inversions (black curve) and in situ by CODIF (red curve). This plot is adapted from C: Son Brandt et al. [2005, JGR, submitted].*

Figure 4 presents HENA Hydrogen image and its corresponding inversion at 17:41 UT, for the 27 to 39 keV energy range. This ENA energy channel corresponds to the upper energy range of CODIF. The ENA image is shown in the upper panel. The Earth is shown as the circle and dipole field-line pairs are shown for L=4 and 8 for midnight, dusk, noon and dawn. The middle panel in Figure 4 shows the image inversion result. The resulting proton distribution is plotted in an L-MLT system and black track is plotted annotating the Cluster spacecraft track, projected on this system at different times. The black dots indicate the Cluster position at different times (in L-MLT coordinates). The lower panel represents a flux comparison between HENA image inversions (black curve) and CODIF in situ measurements (red curve).
According to these inversions, the ring current bulk seem to be centred near the pre-midnight sector, at about MLT=23.

6. DISCUSSION

Since during this event Cluster is situated within the HENA field-of-view, and in order to check the validity of the simultaneous use of these two types of measurements, a comparison of the flux obtained in-situ and the one obtained onboard IMAGE during Cluster equatorial pass (18:00 UT) was suitable. This allows checking the constituency of the results obtained by the inversion method for this particular event, even if the method has already been validated on a statistical basis [10]. *Brandt et al.* [2005, JGR, submitted] compared proton flux for the 27 to 39 keV energy range, which is the overlapping energy range of the two instruments (see fig. 4 (c)). During this pass, the CODIF background due to penetrating particles from the radiation belts is negligible. Furthermore, HENA is well outside the radiation belts. As shown in figure 4 (c), the two methods give very consistent quantitative results all along the Cluster ring current traversal.

Morphology of the ring current:

At 18:00 UT, while crossing the equator, Cluster is situated exactly into the bulk of the ring current. Forty five minutes later, Cluster appears to be situated at the border of it again, in the Northern Hemisphere (fig.2).
Looking at the 27 to 39 keV energy range and judging from fig 2(b) and fig 4(c), we can see that CODIF is recording a large flux increase (one order of magnitude) at 17:15 UT. This appears simultaneously on the HENA inversions. Also, during the outbound pass of the spacecraft, the constellation seems to exit the ring current region between 18:45 UT and 19:00 UT. This is also consistent with HENA inversions. External boundaries are thus extremely well reproduced by the inversion method.

Since the boundaries of the ring current bulk, as deduced from the HENA image inversions, are very consistent with the one observed in-situ by Cluster, and since the two ways of getting ion fluxes presents a very good agreement, we can reasonably use HENA image inversions to get a 2D mapping of the ring current population (for the selected energy range) into the equatorial plane. It appears then clearly that Cluster is traversing the ring current bulk during its perigee pass, even if situated slightly westward of the bulk centre.
This relative azimuthal positioning of Cluster with respect to the ring current bulk (and then with respect to the maximum pressure position) based on the image inversion is then constituent with the curlometer technique.

However, on the contrary the curlometer technique, the inversions seem to show that the maximum proton flux is situated tailward of the Cluster location. This inconsistency can be partially explained by the fact that the $\nabla\vec{P}$ (calculated from curlometer technique) provides a relative positioning of the spacecraft with respect to the maximum pressure created by all particles, not only for the limited protons population with energies between 27 and 39 keV. Thus, if we consider that ring current particles have energies from about 15 keV to 250 keV [24], most part of them are not represented in this particular inversion sequence (which shows only the low energy part of the ring current population). Moreover, as it has been stated in the past [1], maximum ring current pressure is expected to be centered at geocentric distances of the order of ~3 R_E during recovering phases, i.e. earthward with respect to the Cluster perigee position. This is consistent with the curlometer results.

7. CONCLUSIONS

Simultaneous measurements by Cluster (in-situ) and IMAGE (ENA imaging) have provided a unique opportunity to study the 3D mapping of the current for the 20 April 2002 storm time event.
On the one hand, magnetic field data have provided an estimate of the current density (strength and orientation) along the cluster orbit. These data have shown that near the external boundaries between the ring current and the inner plasma sheet, currents issued from different sheets are mixed. This leads to a “filamentation” structure of the three current density components.

The curlometer results revealed also the southward orientation of the current along the Cluster ring current pass, which is possibly the consequence of the different conductivities between the two hemispheres, leading to a most efficient current flow into the Southern hemisphere.

The curlometer revealed the large latitudinal extent (from Ilat=62.5° in the Southern Hemisphere to Ilat=61.8° in the Northern Hemisphere) of the ring current, and it gradual transition from mainly azimuthally flowing current to a more structured one a higher latitude, characterized by the presence of thin current sheets.

On the other hand, remote sensing data, as supplied by energetic neutral atom imaging, is providing a mapping of the equatorial ion distribution.

By comparing flux values obtained in situ by Cluster (while crossing the equatorial plane) and image inversion, we get very consistent values for the 27 to 39 keV energy range.

Moreover, for this energy range, outer boundaries of the ring current particles are very well reproduced by the inversions, for the inbound as well as for the outbound passes of Cluster.

These complementary data are providing, for the first time, an instantaneous mapping of the ring current in 3 dimensions. Using HENA image inversions over a wider energy range together with the curlometer technique, we will be able to deduce the global particle pressure distribution in the equatorial plane, and thus a 3D mapping of the ring current density will be feasible.

REFERENCES

[1] Lui, A. T. Y., R. W. McEntire, S. M. Krimigis, Evolution of the Ring Current during two geomagnetic storms, *J. Geophys. Res.*, 92, No A7, 7459-7470,1987.

[2] Iijima, T., T. A. Potemra, The amplitude distribution of field-aligned currents at northern high latitudes observed by Triad, *J. Geophys. Res.*, Vol. 81 , No. 13 , p. 2165-2174 , 1976.

[3] Robert, P., and A. Roux, Dependence of the shape of the tetrahedron on the accuracy of the estimate of the current density, *in Spatio-temporal Analysis for Resolving Plasma Turbulence* (START), Eur. Space Agency WPP, ESA WPP-047, 289-293, 1993.

[4] Robert, P., Roux , A., Harvey, C. C., Dunlop, M., Daly, P. W., Glassmeier, K.-H.; Tetrahedron Geometric Factors, Analysis Methods for Multi-Spacecraft data, *ISSI Sci. Rep*. SR-001, p. 323-348, 1998.

[5] Dunlop, M. W., Southwood, D. J., Glassmeier, K. -H., Neubauer, F. M, Analysis of multipoint magnetometer data, *Adv. Space Res.*, Vol 8 , No. 9-10 , pp. (9)273 , 1988.

[6] Dunlop, M. W., and A. Balogh, On the analysis and interpretation of four spacecraft magnetic field measurements in terms of small scale plasma processes, in *Spatio-temporal Analysis for Resolving Plasma Turbulence (START), Eur. Space Agency, WPP*, ESA WPP-047, 223, 1993.

[7] C. Vallat, I. Dandouras, M. Dunlop, A. Balogh, E. Lucek, G. K. Parks, M. Wilber, E. C. Roelof, G. Chanteur, H. Rème, First current density measurements in the ring current region using simultaneous multi-spacecraft CLUSTER-FGM data, *Ann. Geophys.*, 23,1849-1865, 2005.

[8] DeMajistre, R., E. C. Roelof, P. C:son Brandt, and D. G. Mitchell, Retrieval of global magnetospheric ion distributions from high-energy neutral atom measurements made by the IMAGE/HENA instrument, *J. Geophys. Res.*, *109*, A04214, doi:10.1029, 2004

[9] C:son Brandt, P., R. DeMajistre, E. C. Roelof, D. G. Mitchell, and S. Mende, IMAGE/HENA: Global ENA imaging of the plasmasheet and ring current during substorms, *J. Geophys. Res*., 107, SMP 21-1 to SMP 21-13, 2002

[10] Vallat, C., I. Dandouras, P. C:Son. Brandt, R. DeMajistre, D. G. Mitchell, E. C. Roelof, H. Rème, J.-A. Sauvaud, L. Kistler, C. Mouikis, M. Dunlop, A. Balogh, First comparisons of local ion measurements in the inner magnetosphere with energetic neutral atom magnetospheric image inversions: Cluster-CIS and IMAGE-HENA observations, *J. Geophys. Res*., 109, A04213, doi 10.1029, 2004.

[11] Williams, D.J., E.C. Roelof, and D.G. Mitchell, Global Magnetospheric Imaging, *Rev. Geophys*., 30,183,1992.

[12] Tsyganenko, N. A., H. J. Singer, and J. C. Kasper, Storm-time distortion of the inner magnetosphere: How severe can it get?, *J. Geophys.Res.*,*108*(A5),1209, doi:10.1029, 2003.

[13] Østgaard, N., S.B. Mende, H.U. Frey, G.R. Gladstone, H. Lauche, Neutral hydrogen density profiles derived from geocoronal imaging, *J. Geophys. Res*, vol 108, No A7, 1300, 2003.

[14] Twomey, S., Introduction to the mathematics in remote sensing and indirect measurements, Developments in *geomathematics 3, 1st ed., Elsevier scientific publishing company*, 1977.

[15] Rodgers, C., *Inverse Methods for Atmospheric Sounding*, World Scientific, 2000.

[16] Menke, W., Geophysical Data Analysis: Discrete Inverse Theory, *Academic Press Inc*., 1989.

[17] Escoubet, C.P., M. Fehringer, M. Goldstein, The Cluster mission, *Ann. Geophys.*, 19,1197-1200, 2001.

[18] Rème, H., C. Aoustin, J. Bosqued, I. Dandouras, B. Lavraud, J.A Sauvaud, A. Barthe, J. Bouyssou, Th. Camus, O. Coeur-Joly, et al., First multispacecraft ion measurements in and near the Earth's magnetosphere with the identical Cluster ion spectrometry (CIS) experiment, *Ann. Geophysicae*, 19, 1303-1354, 2001.

[19] Balogh, A., et al., The Cluster Magnetic Field Investigation: Overview of in-flight performance and initial results, *Ann. Geophys*.; 19, 1207-1217, 2001.
[20] Burch, J.L., (Ed), *The IMAGE Mission*, Kluwer Acad., Norwell, Mass., 2000 (Reprinted from Space Sci. Rev., 91, 2000.)
[21] Mitchell, D.G., et al., High-energy neutral atom (HENA) imager for the IMAGE mission, *Space Sci. Rev*., 91, 67-112, 2000.
[22] Hurtaud, Y., Modélisation de la dynamique couplée des plasmas magnétosphérique et ionosphérique, *rapport de stage de DEA*, CESR, Toulouse, 2004.
[23] Lu, G.; A. D.Richmond; B. A.Emery; P. H .Reiff; O. de La Beaujardiere; F. J. Rich; W. F. Denig; H. W. Kroehl; L. R. Lyons; J. M. Ruohoiemi, Interhemispheric asymmetry of the high-latitude ionospheric convection pattern, *J. Geophys. Res*, Vol. 99, no. A4, p. 6491-6510, 1994.
[24] Williams, D. J., Ring current and radiation belts, *U. S. Natl. Rep. Int. Union Geod. Geophys.* 1983-1986, *Rev Geophys*., 25, 570-578, 1987.